Automatic Carrier Landing Control for Unmanned Aerial Vehicles Based on Preview Control

Zhen Ziyang[1,2*], *Ma Kun*[2], *Bhatia Ajeet Kumar*[2]

1. College of Automation Engineering, Nanjing University of Aeronautics and Astronautics, Nanjing 210016, P. R. China
2. Jiangsu Key Laboratory of Internet of Things and Control Technologies, Nanjing 210016, P. R. China

(Received 1 September 2016; revised 6 December 2016; accepted 14 February 2017)

Abstract: For carrier-based unmanned aerial vehicles (UAVs), one of the important problems is the design of an automatic carrier landing system (ACLS) that would enable the UAVs to accomplish autolanding on the aircraft carrier. However, due to the movements of the flight deck with six degree-of-freedom, the autolanding becomes sophisticated. To solve this problem, an accurate and effective ACLS is developed, which is composed of an optimal preview control based flight control system and a Kalman filter based deck motion predictor. The preview control fuses the future information of the reference glide slope to improve landing precision. The reference glide slope is normally a straight line. However, the deck motion will change the position of the ideal landing point, and tracking the ideal straight glide slope may cause landing failure. Therefore, the predictive deck motion information from the deck motion predictor is used to correct the reference glide slope, which decreases the dispersion around the desired landing point. Finally, simulations are carried out to verify the performance of the designed ACLS based on a nonlinear UAV model.

Key words: carrier-based unmanned aerial vehicles; optimal preview control; automatic carrier landing system; deck motion predictor

CLC number: V249 **Document code**: A **Article ID**: 1005-1120(2017)04-0413-07

0 Introduction

In the foreseeable future war, UAVs will play an increasingly important role. For the military applications of the carrier-based UAVs, carrier autolanding presents one of the most critical problems[1-2]. Approaching and descending to a ship deck with small dimensions is a very difficult task for the UAVs, especially when the ship deck irregularly moves due to the influence of ocean wave[3-4]. Therefore, a reliable automatic carrier landing system(ACLS) is necessary for the UAVs, which can reduce operating costs (No need for a skilled RC pilot) and improve the security of recovery[5]. Generally, the carrier-based UAVs accomplish automatic carrier landing by tracking the pre-designed glide slope, which is the flight path of the UAVs from the approach point to the landing point[6]. Due to the irregular deck motion, the desired landing point changes randomly. Especially the longitudinal deck motion can change the ideal landing height, which may cause the UAVs unable to landing safely. Therefore, research on ACLS with deck motion compensation is important.

Many researches have been developed for several decades. Most of them focused on classical and robust linear control methods[7-8]. Some researchers used the nonlinear control methods to design the flight control systems for the nonlinear UAVs[9-10]. However, it is sporadic that the foreseeable glide slope information is used to improve the landing accuracy. To eliminate the influence of deck motion, current researches mainly focus on the establishment of the phase advance network. But these methods cannot eliminate the

* Corresponding author, E-mail address: zhenziyang@nuaa.edu.cn.

How to cite this article: Zhen Ziyang, Ma Kun, Bhatia Ajeet Kumar. Automatic carrier landing control for unmanned aerial vehicles based on preview control[J]. Trans. Nanjing Univ. Aero. Astro., 2017,34(4):413-419.
http://dx.doi.org/10.16356/j.1005-1120.2017.04.413

phase lag of the system effectively because of the limited compensation ability of the advanced network itself.

Differing from the above researches, this paper presents a preview control method to solve the autolanding control problem of the UAVs. The development of the preview control theory is given in Ref. [11]. The main contributions of this paper are as follows:

(1) The foreseeable glide slope future information is used by the optimal preview control to improve the tracking accuracy, in which the optimal preview controller is composed of a state feedback controller and a foreseeable reference information feedforward controller. Simulations of a nonlinear UAV model verify the high landing precision of the preview control method.

(2) To correct the reference glide slope information under the influence of the carrier deck motion, the combination of an optimal preview control based flight control system and a Kalman filter based deck motion predictor is developed. Simulation results show that the combination strategy can improve the landing accuracy effectively.

1 Formulation and Preliminaries

The automatic carrier landing problem of the UAVs is formulated. Preliminaries of the deck motion model and the optimal preview control are also given.

1.1 Problem statement

The automatic carrier landing problem is described as:

(1) Guidance and flight control problem: Once the UAVs fly off the reference glide slope, the guidance system is needed to generate attitude commands according to the tracking error, and the flight control system is needed to adjust the flying attitude of the UAVs after receiving the attitude commands, and to eliminate tracking error eventually.

(2) Deck motion prediction problem: The irregular deck motion can change the position of the landing point, and the reference glide slope should thus be corrected, which means the future information of the deck motion needs to be fused to the reference glide slope, therefore, an accurate deck motion predictor is necessary.

1.2 Deck motion model

A large number of experimental observations and data analysis show that the ocean wave motion is a stationary stochastic process. Since the ship can be regarded as a linear system in a certain condition, the deck motion also is a stationary stochastic process[12]. Hence, we can use the power spectral density function curve of the deck motion to find the optimal coefficients of the deck motion shaping filter $G(s)$, and then the time domain information of the deck motion is obtained when the white noise is filtered through the deck motion shaping filter. According to Ref. [12], $G(s)$ has the following expression

$$G(s)=\frac{as^2}{s^4+bs^3+cs^2+ds+e} \tag{1}$$

In practice, the power spectral density function curve of the deck motion can be obtained by a large number of experiments and simulations in the sea or pool, then the coefficients of $G(s)$ are obtained by calculating the power spectral density function curve.

1.3 Optimal preview control theory

By using the reference information as feedforward control signal, the optimal preview control can reduce input energy and improve respond time effectively. Generally, the optimal preview control problems can be categorized into two types depending on the "previewed signal": either the desired trajectory in a tracking problem, or the external disturbance signal in a regulating problem[13].

Obviously, the automatic carrier landing problem is a trajectory tracking problem, in which the desired trajectory is the reference glide slope information. Therefore, the preview control theory is adopted to solve the reference glide slope tracking problem of UAVs.

2 Automatic Carrier Landing System Design

The ACLS is mainly composed of a deck motion predictor a flight control system, as shown in Fig. 1. Generally, the flight control system can be separated into two parts: the longitudinal channel and the lateral channel. The preview information for the longitudinal and lateral channels are the reference glide slope height H_c and the reference glide slope lateral bias Y_c, respectively.

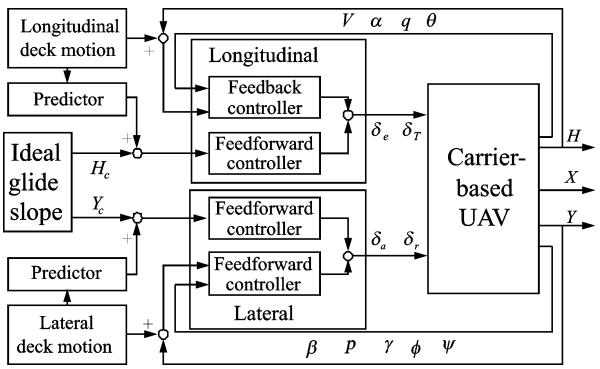

Fig. 1 Structure of ACLS

2.1 Deck motion predictor design

For the linear constant transfer function of the deck motion Eq. (1), by using the minimal realization method, the state space expression of the deck motion can be obtained.

$$\begin{cases}\dot{\boldsymbol{x}}=\boldsymbol{A}\boldsymbol{x}+\boldsymbol{b}w\\ \boldsymbol{z}=\boldsymbol{c}^{\mathrm{T}}\boldsymbol{x}+v\end{cases} \tag{2}$$

where $\boldsymbol{x}=[x_1,x_2,x_3,x_4]^{\mathrm{T}}$, here, x_1 is the deck motion amplitude; x_2, x_3, x_4 are the first derivative, second derivative and third derivative of x_1, respectively. $\boldsymbol{z}$ is the observed signal; $\boldsymbol{w}$ the system dynamic noise; and $\boldsymbol{v}$ the observation noise.

The deck motion predictor is designed based on the discrete Kalman filter theory. Discretizing the deck motion model Eq. (2), we obtain

$$\begin{cases}\boldsymbol{x}_k=\boldsymbol{\Phi}_{k,k-1}\boldsymbol{x}_{k-1}+\boldsymbol{\Gamma}_{k,k-1}\boldsymbol{w}_{k-1}\\ \boldsymbol{z}_k=\boldsymbol{H}_k\boldsymbol{x}_k+\boldsymbol{v}_k\end{cases} \tag{3}$$

The calculation procedure of the deck motion predictor based on the Kalman filter theory and the optimal estimation theory can be devided into two stages. The first step is to calculate the optimal filtering value $\hat{\boldsymbol{x}}_{k|k}$ at time k; and the second step is to predict of deck motion information $\hat{\boldsymbol{x}}_{k+m|k}$ after time τ, where $m=\tau/T_s$. The detailed design process can be found in Ref. [14].

2.2 Optimal preview control law design

Optimal preview control is a linearization based control method, therefore the first step is to build the linear UAV model. By using small perturbation linearization method, the nonlinear UAV model near the trimmed landing flight state can be obtained with the following form.

$$\dot{\boldsymbol{x}}=\boldsymbol{A}\boldsymbol{x}+\boldsymbol{B}\boldsymbol{u} \tag{4}$$

where $\boldsymbol{x}=[\Delta V,\Delta\alpha,\Delta q,\Delta\theta,\Delta\beta,\Delta p,\Delta r,\Delta\phi,\Delta\psi]^{\mathrm{T}}$ is the state vector of the UAV ("Δ" represents the increment near the trim point of the state), encompassing airspeed, attack angle, pitch rate, pitch angle, sideslip angle, roll rate, yaw rate, roll angle, and yaw angle in sequence. $\boldsymbol{u}=[\Delta\delta_e,\Delta\delta_T,\Delta\delta_a,\Delta\delta_r]^{\mathrm{T}}$ is the control vector of elevator angle, throttle opening, aileron angle and rudder angle. $\boldsymbol{A}$ and $\boldsymbol{B}$ are the state coefficient matrices.

Decoupling the linear UAV model into the longitudinal and the lateral channels, we get

$$\dot{\boldsymbol{x}}_{\mathrm{lon}}=\boldsymbol{A}_{\mathrm{lon}}\boldsymbol{x}_{\mathrm{lon}}+\boldsymbol{B}_{\mathrm{lon}}\boldsymbol{u}_{\mathrm{lon}} \tag{5}$$

$$\dot{\boldsymbol{x}}_{\mathrm{lat}}=\boldsymbol{A}_{\mathrm{lat}}\boldsymbol{x}_{\mathrm{lat}}+\boldsymbol{B}_{\mathrm{lat}}\boldsymbol{u}_{\mathrm{lat}} \tag{6}$$

where $\boldsymbol{x}_{\mathrm{lon}}=[\Delta V,\Delta\alpha,\Delta q,\Delta\theta]^{\mathrm{T}}$ is the longitudinal state vector; $\boldsymbol{u}_{\mathrm{lon}}=[\Delta\delta_e,\Delta\delta_T]^{\mathrm{T}}$ the longitudinal control vector; $\boldsymbol{x}_{\mathrm{lat}}=[\Delta\beta,\Delta p,\Delta r,\Delta\varphi,\Delta\psi]^{\mathrm{T}}$ the lateral vector; $\boldsymbol{u}_{\mathrm{lat}}=[\Delta\delta_a,\Delta\delta_r]^{\mathrm{T}}$ the lateral control vector; and $\boldsymbol{A}_{\mathrm{lon}}$, $\boldsymbol{B}_{\mathrm{lon}}$, $\boldsymbol{A}_{\mathrm{lat}}$ and $\boldsymbol{B}_{\mathrm{lat}}$ the coefficient matrices.

2.2.1 Longitudinal control law design

The longitudinal control system of the UAV automatically adjusts the elevator angle and the throttle opening to control the attitude angle and airspeed, and then makes the UAVs track the scheduled glide slope altitude. The structure diagram of the longitudinal control system is shown in Fig. 2.

For the longitudinal optimal preview controller, the predictable information is the ideal glide slope altitude H_c (The relative altitude refers to the deck). The flight altitude H should be added into the longitudinal model of the UAV.

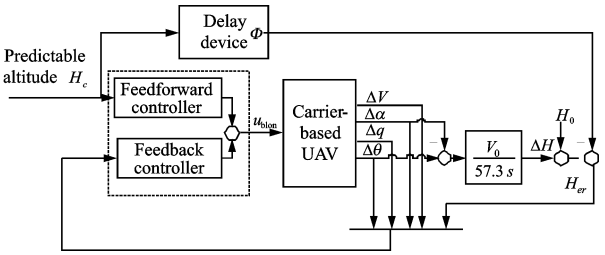

Fig. 2 Structure of longitudinal control system

According to the simplified navigation equation

$$\dot{H} \approx \frac{V}{57.3}(\theta - \alpha) \tag{7}$$

The altitude H is added to the model Eq. (5). The extended longitudinal model of the UAVs can be obtained.

$$\begin{cases} \dot{\boldsymbol{x}}_{\text{blon}} = \boldsymbol{A}_{\text{blon}}\boldsymbol{x}_{\text{blon}} + \boldsymbol{B}_{\text{blon}}\boldsymbol{u}_{\text{blon}} \\ y_{\text{blon}} = \boldsymbol{C}_{\text{blon}}\boldsymbol{x}_{\text{blon}} \end{cases} \tag{8}$$

where $\boldsymbol{x}_{\text{blon}} = [\Delta V, \Delta\alpha, \Delta q, \Delta\theta, \Delta H]^{\text{T}}$ is the state vector, $\boldsymbol{u}_{\text{blon}} = [\Delta\delta_e, \Delta\delta_T]^{\text{T}}$ is the control vector, $y_{\text{blon}} = H$ is the output, and

$$\boldsymbol{A}_{\text{blon}} = \begin{bmatrix} & \boldsymbol{A}_{\text{lon}} & \\ 0 & -\frac{V}{57.3} & 0 \end{bmatrix},\ \boldsymbol{B}_{\text{blon}} = \begin{bmatrix} \boldsymbol{B}_{\text{lon}} \\ 0 \end{bmatrix}$$

$$\boldsymbol{C}_{\text{blon}} = [0 \quad 0 \quad 0]$$

Discretize the extended model Eq. (8) by sampling time $T = 0.1$ s, we attain

$$\begin{cases} \boldsymbol{x}_{\text{blon}}(k+1) = \boldsymbol{A}^*_{\text{blon}}\boldsymbol{x}_{\text{blon}}(k) + \boldsymbol{B}^*_{\text{blon}}\boldsymbol{u}_{\text{blon}}(k) \\ y_{\text{blon}}(k+1) = \boldsymbol{C}^*_{\text{blon}}\boldsymbol{x}_{\text{blon}}(k) \end{cases} \tag{9}$$

Define an error signal

$$e(k) = H_c(k) - y_{\text{blon}}(k) \tag{10}$$

then we get an extended error system.

$$\boldsymbol{X}_{\text{lon}}(k+1) = \boldsymbol{\Phi}_{\text{lon}}\boldsymbol{X}_{\text{lon}}(k) + \boldsymbol{G}_{\text{lon}}\Delta\boldsymbol{u}_{\text{blon}}(k) + \boldsymbol{G}_H\Delta H_c(k+1) \tag{11}$$

where $\boldsymbol{X}_{\text{lon}}(k) = [e(k), \Delta\boldsymbol{x}_{\text{blon}}(k)]^{\text{T}}$, and

$$\boldsymbol{\Phi} = \begin{bmatrix} \boldsymbol{I} & -\boldsymbol{C}^*_{\text{blon}}\boldsymbol{A}^*_{\text{blon}} \\ 0 & \boldsymbol{A}^*_{\text{blon}} \end{bmatrix},\ \boldsymbol{G} = \begin{bmatrix} -\boldsymbol{C}^*_{\text{blon}}\boldsymbol{B}^*_{\text{blon}} \\ \boldsymbol{B}^*_{\text{blon}} \end{bmatrix},$$

$$\boldsymbol{G}_H = \begin{bmatrix} \boldsymbol{I} \\ 0 \end{bmatrix}$$

According to the optimal preview control theory, an optimal preview controller can be designed as

$$\Delta\boldsymbol{u}_{\text{blon}}(k) = \boldsymbol{F}_0\boldsymbol{X}_{\text{lon}}(k) + \sum_{j=0}^{M_R}\boldsymbol{F}_H(j)\Delta H_c(k+j) \tag{12}$$

where the state feedback and the preview feedforward coefficients are

$$\boldsymbol{F}_0 = -[\boldsymbol{R} + \boldsymbol{G}^{\text{T}}\boldsymbol{P}\boldsymbol{G}]^{-1}\boldsymbol{G}^{\text{T}}\boldsymbol{P}\boldsymbol{\Phi}$$

$$\begin{cases} \boldsymbol{F}_H(0) = 0 \\ \boldsymbol{F}_H(j) = -[\boldsymbol{R} + \boldsymbol{G}^{\text{T}}\boldsymbol{P}\boldsymbol{G}]^{-1}\boldsymbol{G}^{\text{T}}(\boldsymbol{\xi}^{\text{T}})^{j-1}\boldsymbol{P}\boldsymbol{G}_H \quad (j \geqslant 1) \\ \boldsymbol{\xi} = \boldsymbol{\Phi} + \boldsymbol{G}\boldsymbol{F}_0 \end{cases}$$

and $\boldsymbol{P}$ satisfies the matrix-difference-Riccati equation

$$\boldsymbol{P} = \boldsymbol{Q} + \boldsymbol{\Phi}^{\text{T}}\boldsymbol{P}\boldsymbol{\Phi} - \boldsymbol{\Phi}^{\text{T}}\boldsymbol{P}\boldsymbol{G}[\boldsymbol{R} + \boldsymbol{G}^{\text{T}}\boldsymbol{P}\boldsymbol{G}]^{-1}\boldsymbol{G}^{\text{T}}\boldsymbol{P}\boldsymbol{\Phi}$$

where the weight matrices $\boldsymbol{Q}$, $\boldsymbol{R}$ and preview step number M_R are the adjustable parameters.

Considering the influence of the deck motion, the ideal height H_c is changed to $\widetilde{H}_c$.

$$\widetilde{H}_c = H_c + \Delta Z_{\text{he}} \tag{13}$$

where ΔZ_{he} is the estimated future value of the deck motion, which can be obtained from Section 2.1.

2.2.2 Lateral control law design

The lateral control system of the UAV automatically adjusts the aileron and the rudder to control the roll angle, and continues to correct the flight path azimuth angle until lateral error becomes zero.

For the lateral preview controller, the predictable information (Reference signal) is the ideal glide slope lateral bias Y_c. The lateral preview controller has the similar structure as the longitudinal preview controller. The lateral preview control law can be designed as

$$\Delta\boldsymbol{u}_{\text{blat}}(k) = \boldsymbol{F}^*_0\boldsymbol{X}_{\text{lat}}(k) + \sum_{j=0}^{M_R}\boldsymbol{F}_Y(j)\Delta Y_c(k+j) \tag{14}$$

where

$$\boldsymbol{X}_{\text{lat}}(k) = [e(k), \Delta x_{\text{blat}}(k)]^{\text{T}},\ \boldsymbol{u}_{\text{blat}} = [\Delta\delta_a, \Delta\delta_r]^{\text{T}}$$

$$\boldsymbol{F}^*_0 = -[\boldsymbol{H} + \boldsymbol{G}^{\text{T}}_{\text{lat}}\boldsymbol{P}\boldsymbol{G}_{\text{lat}}]^{-1}\boldsymbol{G}^{\text{T}}_{\text{lat}}\boldsymbol{P}\boldsymbol{\Phi}_{\text{lat}}$$

$$\begin{cases} \boldsymbol{F}_Y(0) = 0 \\ \boldsymbol{F}_Y(j) = -[\boldsymbol{H} + \boldsymbol{G}^{\text{T}}_{\text{lat}}\boldsymbol{P}\boldsymbol{G}_{\text{lat}}]^{-1}\boldsymbol{G}^{\text{T}}_{\text{lat}}(\boldsymbol{\xi}^{\text{T}})^{j-1}\boldsymbol{P}\boldsymbol{G}_Y (j \geqslant 1) \end{cases}$$

$$\boldsymbol{\xi} = \boldsymbol{\Phi}_{\text{lat}} + \boldsymbol{G}_{\text{lat}}\boldsymbol{F}^*_0,\ \boldsymbol{\Phi}_{\text{lat}} = \begin{bmatrix} \boldsymbol{I} & -\boldsymbol{C}^*_{\text{blat}}\boldsymbol{A}^*_{\text{blat}} \\ 0 & \boldsymbol{A}^*_{\text{blat}} \end{bmatrix}$$

$$\boldsymbol{G}_{\text{lat}} = \begin{bmatrix} -\boldsymbol{C}^*_{\text{blat}}\boldsymbol{B}^*_{\text{blat}} \\ \boldsymbol{B}^*_{\text{blat}} \end{bmatrix},\ \boldsymbol{G}_Y = \begin{bmatrix} \boldsymbol{I} \\ 0 \end{bmatrix}$$

$$\boldsymbol{P} = \boldsymbol{Q} + \boldsymbol{\Phi}^{\text{T}}_{\text{lat}}\boldsymbol{P}\boldsymbol{\Phi}_{\text{lat}} - \boldsymbol{\Phi}^{\text{T}}_{\text{lat}}\boldsymbol{P}\boldsymbol{G}_{\text{lat}}[\boldsymbol{H} + \boldsymbol{G}^{\text{T}}_{\text{lat}}\boldsymbol{P}\boldsymbol{G}_{\text{lat}}]^{-1}\boldsymbol{G}^{\text{T}}_{\text{lat}}\boldsymbol{P}\boldsymbol{\Phi}_{\text{lat}}$$

3 Simulation

The proposed ACLS based on preview con-

trol is applied to a nonlinear UAV model here, and the controlling performance is verified by comparing with the traditional linear quadratic (LQ) optimal control method.

3.1 Simulation conditions

The UAV chosen as a prototype for the research is "Silver Fox"[15]. The initial state variable values of the UAV are shown in Table 1.

Table 1 Initial state values of UAV

Parameter	Value	Parameter	Value
V/ (m · s^{-1})	20	φ/ (°)	0
α/ (°)	3.959	ψ/ (°)	0
q/ ((°) · s^{-1})	0	δ_e/ (°)	−3.994
θ/ (°)	0.458 4	δ_T/%	44.07
β/ (°)	0	δ_a/ (°)	0
p/ ((°) · s^{-1})	0	δ_r/ (°)	0
r/ ((°) · s^{-1})	0	h/ m	19

Linearizing the nonlinear UAV model in the balanced flight state, the linear models are given by

$$\boldsymbol{A}_{\text{lon}} = \begin{bmatrix} -0.084\ 3 & 6.029\ 2 & -1.648\ 4 & -9.781\ 7 \\ -0.048\ 8 & -3.991\ 9 & -0.738\ 6 & 0.029\ 9 \\ 0.033\ 9 & -96.978\ 1 & -260.250\ 4 & 0 \\ 0 & 0 & 1 & 0 \end{bmatrix}$$

$$\boldsymbol{B}_{\text{lon}} = \begin{bmatrix} -2.165\ 7 & \\ -0.575\ 0 & \\ -95.559\ 6 & \\ 0 & 2.056\ 0 \\ -0.007\ 1 & \\ 0 & \\ 0 & \end{bmatrix}$$

$$\boldsymbol{A}_{\text{lat}} = \begin{bmatrix} -0.179\ 8 & 0.069 & -0.997\ 6 & 0.49 & 0 \\ -22.456\ 5 & -8.213 & 2.004\ 6 & 0 & 0 \\ 15.074\ 7 & -0.657\ 8 & -0.709\ 5 & 0 & 0 \\ 0 & 1 & 0.008 & 0 & 0 \\ 0 & 0 & 1 & 0 & 0 \end{bmatrix}$$

$$\boldsymbol{B}_{\text{lon}} = \begin{bmatrix} 0 & 0.087\ 3 \\ 99.514\ 4 & 2.403\ 4 \\ -7.939\ 7 & -10.112\ 4 \\ 0 & 0 \\ 0 & 0 \end{bmatrix}$$

In this simulation, the sampling time of the preview controller is 0.1 s, the preview step number is 20, the inclination angle of the glide slope is −3.5°, the initial altitude deviation is 1 m, and the initial lateral deviation is 1 m. For the deck motion model, the sample time is 0.1 s. The white noise is set as: the noise powers of the system dynamic noise $\boldsymbol{w}$ and the observation noise $\boldsymbol{v}$ are 1.0 and 0.225, respectively.

3.2 Simulation results

Figs. 3, 4 show the simulation results of the proposed automatic landing control system without considering the influence of deck motion. Figs. 5—8 are the simulation results under the influence of deck motion, where the control methods in Fig. 5(a) and Fig. 7(a) are based on the LQ control, while Fig. 5(b) and Fig. 7(b) are based on the optimal preview control. Fig. 6 and Fig. 8 are the tracking error curves.

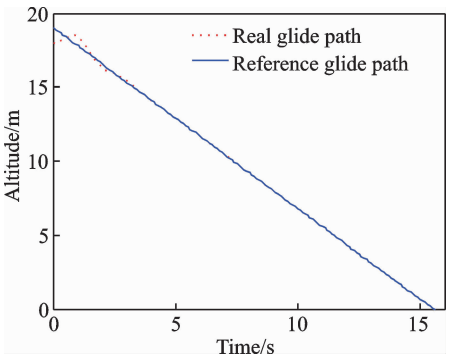

Fig. 3 Longitudinal tracking curve

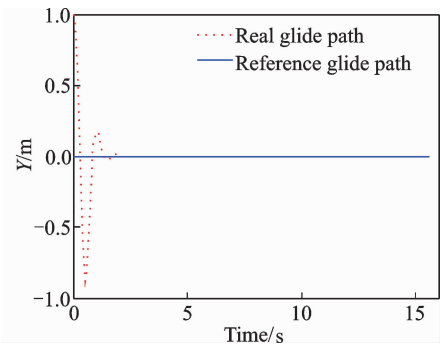

Fig. 4 Lateral tracking curve

Viewing from Figs. 3, 4, it is founded that the proposed control system can effectively control the UAV to track the ideal glide slope when there is no deck motion influence. From Figs. 5—8, it is found that the optimal preview controller

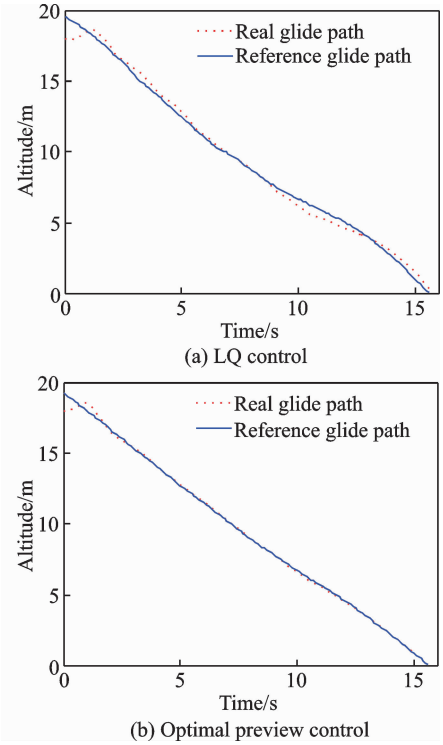

Fig. 5 Longitudinal tracking curve with deck motion

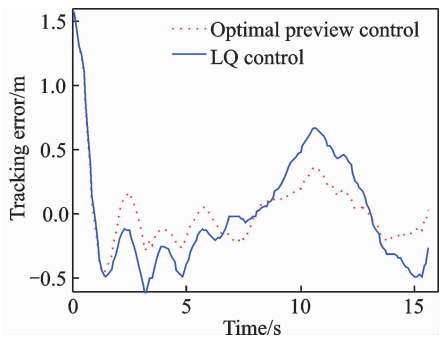

Fig. 6 Longitudinal tracking error curve

has smaller tracking error than the traditional LQ controller, which means the proposed method can effectively improve the success rate of the carrier landing for the UAVs. This is due to the effective use of the preview feedforward information.

4 Conclusions

An optimal preview control based ACLS is proposed to guide the UAV to accurate tracking of the reference glide slope and compensate the deck motion disturbance. The proposed control method can effectively utilize the future reference glide slope information, which has not been studied yet. Simulation results of a nonlinear UAV model show that the optimal preview control method has faster response time and higher accuracy than the traditional LQ control method.

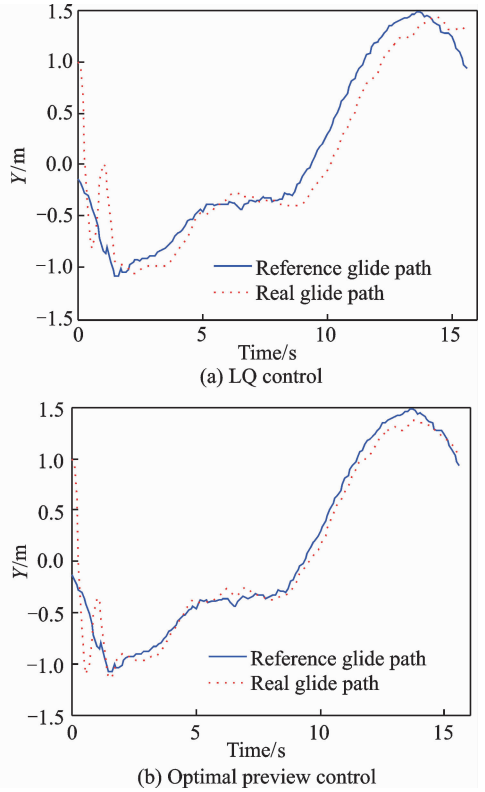

Fig. 7 Lateral tracking curve with deck motion

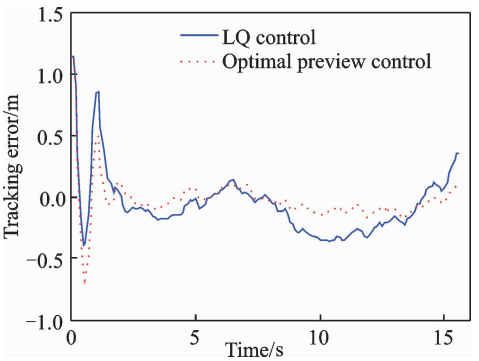

Fig. 8 Lateral tracking error curve

Acknowledgments

This work was supported in part by the National Natural Science Foundations of China (Nos. 61304223, 61673209, 61533008), the Aeronautical Science Foundation (No. 2016ZA 52009), and the Fundamental Research Funds for the Central Universities (No. NJ20160026).

References:

[1] BOSKOVIC J, REDDING J. An autonomous carrier landing system for unmannned aerial vehicles[C]//

AIAA Guidance, Navigation, and Control Conference. [S. l.]: AIAA, 2009.

[2] PU H Z, ZHEN Z Y, XIA M. Flight control system of unmanned aerial vehicle[J]. Transactions of Nanjing University of Aeronautics and Astronautics, 2015, 32(1): 1-8.

[3] STORVIK M. Guidance system for automatic approach to a ship[D]. Trondheim, Norwegian: Norwegian University of Science and Technology, 2003.

[4] YANG Y D, ZHEN Z Y, QIU S B, et al. UAV carrier landing guidance and control[M]. Beijing: National Defense Industry Press, 2013.

[5] SKULSTAD R, SYVERSEN C L, MERZ M, et al. Net recovery of UAV with single-frequency RTK GPS [C]// Aerospace Conference. [S. l.]: IEEE, 2015.

[6] WANG S, ZHEN Z Y, JIANG J, et al. Flight tests of autopilot integrated with fault-tolerant control of a small fixed-wing UAV[J]. Mathematical Problems in Engineering, 2016(1): 1-7.

[7] CRASSIDIS J, MOOK D. Robust control design of an automatic carrier landing system[C]// Astrodynamics Conference. [S. l.]: AIAA, 1992.

[8] JASON W, GREGPRY T, ROBERT R. Adaptive flight control of a carrier based unmanned air vehicle [C]//AIAA Guidance, Navigation, and Control Conference and Exhibit. Austin, Texas: [s. n.], 2003.

[9] ZHENG F Y, GONG H J, ZHEN Z Y. Adaptive constraint backstepping fault-tolerant control for small carrier-based unmanned aerial vehicle with uncertain parameters[J]. Proceedings of the Institution of Mechanical Engineers Part G: Journal of Aerospace Engineering, 2016, 230: 407-425.

[10] STEINBERG M. A fuzzy logic based F/A-18 automatic carrier landing system[C]// Guidance, Navigation and Control Conference. [S. l.]: AIAA, 2012.

[11] ZHEN Z Y. Research progress of preview control theory and application[J]. Acta Automatica Sinica, 2016, 42(2): 172-188.

[12] WANG J. Control principle of ocean moving body [M]. Harbin: Harbin Institute of Technology Press, 2007.

[13] PENG H, TOMIZUKA M. Optimal preview control for vehicle lateral guidance, PATH Research Report UCB-ITS-PRR-91-16[R]. 1991.

[14] ZHANG Y, ZHOU X. Research on longitudinal deck motion compensation[J]. Electronics Optics & Control, 2012, 19(4): 18-22.

[15] MARIANO I L. Autonomous landing system for a UAV[D]. Monterey, California: Naval Postgraduate School, 2004.

Dr. **Zhen Ziyang** received his Ph. D. degree from the Nanjing University of Aeronautics and Astronautics (NUAA) in 2010. He worked at the University of Virginia in USA as a visiting scholar during February 2015 and February 2016. Currently, he is working at NUAA as an associate professor. His research interests cover advanced flight control of carrier-based aircrafts, hypersonic aircrafts and UAVs formation, adaptive control and preview control.

Mr. **Ma Kun** received his B. Sc. degree from the School of Automation, NUAA in 2014. He is currently a master student in NUAA. His research interests focus on flight control and preview control theory.

Mr. **Bhatia Ajeet Kumar** received his B. Sc. degree from Quaid-e-Awam University of Engineering Science and Technology (QUEST), Nawabshah, Pakistan in 2009. He is currently a postgraduate student in NUAA. He is also junior engineer in Pakistan Council of Scientific and Industrial Research (PCSIR) laboratories complex, Karachi.

(Executive Editor: Zhang Tong)